PROCEEDINGS OF SCIENCE

Deep Neural Networks for combined neutrino energy estimate with KM3NeT/ORCA6

Santiago Peña Martínez[a,*] **on behalf of the KM3NeT Collaboration**

[a] *Université Paris Cité, CNRS, Astroparticule et Cosmologie, F-75013 Paris, France*

E-mail: spenam@apc.in2p3.fr

KM3NeT/ORCA is a large-volume water-Cherenkov neutrino detector, currently under construction at the bottom of the Mediterranean Sea at a depth of 2450 meters. The main research goal of ORCA is the measurement of the neutrino mass ordering and the atmospheric neutrino oscillation parameters. Additionally, the detector is also sensitive to a wide variety of phenomena including non-standard neutrino interactions, sterile neutrinos, and neutrino decay.

This contribution describes the use of a machine learning framework for building Deep Neural Networks (DNN) which combine multiple energy estimates to generate a more precise reconstructed neutrino energy. The model is optimized to improve the oscillation analysis based on a data sample of 433 kton-years of KM3NeT/ORCA with 6 detection units. The performance of the model is evaluated by determining the sensitivity to oscillation parameters in comparison with the standard energy reconstruction method of maximizing a likelihood function. The results show that the DNN is able to provide a better energy estimate with lower bias in the context of oscillation analyses.

38th International Cosmic Ray Conference (ICRC2023)
26 July - 3 August, 2023
Nagoya, Japan

*Speaker

PoS(ICRC2023)1035

1. Introduction

KM3NeT is a neutrino telescope under construction in the Mediterranean Sea [1]. It consists of two water-Cherenkov detectors: ARCA and ORCA. The principle of detection uses the Cherenkov light induced by charged particles produced in neutrino interactions in the water. The emitted light is collected by an array of photomultiplier tubes (PMTs) housed in glass spheres to form digital optical modules (DOMs). Each DOM holds 31 PMTs arranged to provide directional information of the incoming photons. The ORCA detector will consist of 115 detection units (DUs) instrumented with 2070 DOMs, with a total volume of about 7 Mton. The main goal of ORCA is to determine the neutrino mass ordering and the atmospheric neutrino oscillation parameters. For this analysis, Monte Carlo (MC) simulations from an early detector configuration with 6 DUs are used.

The reconstruction of the neutrino energy is a key aspect for the oscillation analysis of KM3NeT/ORCA. Current methods for the energy reconstruction are based on the maximization of a likelihood function, which relies on a hypothesis for the distribution of light from a neutrino interaction. This distribution is either track-like when it is induced by muons or shower-like when it is generated by an electromagnetic or hadronic cascade of charged secondary particles. However, this approach has some limitations. For the case of the track-like topology, it is assumed for the reconstruction that the muon propagates in a straight line without scattering. For the shower-like topology, the produced lepton is e.g. an electron which will induce an electromagnetic cascade that is assumed to induce light emission in a sperically symmetric way. Both of the hypotheses do not cover the full picture of the interaction. When a neutrino interacts with a nucleus it produces not only an outgoing lepton but also a shower of hadrons that will induce light.

The present study aims to make use of the current energy estimates which rely on the track and shower hypotheses, and combines them with extra auxiliary information, such as the number of triggered hits, to consider the full information of the interaction topology. By using this ancillary information and the energy estimates from each hypothesis (track-like, shower-like, and the track length as an energy proxy) as an input, a Deep Neural Network (DNN), which outputs an improved energy estimate, is built. The training of the DNN is done using MC simulations of atmospheric neutrinos. In order to create the network, a set of hyperparameters has to be selected. The hyperparameters consist of configuration settings that the network cannot learn by itself, such as the number of layers, the number of neurons per layer, the activation function, and the loss function. The values of all of these hyperparameters have to be optimized in order to obtain the best possible network for the given problem.

The best set of hyperparameters will be determined by the performance of the network on validation data with respect to a chosen metric. For standard regression problems in machine learning, the metric used is the mean squared error (MSE). In general, the network should be trained for the lowest possible MSE. However, this might not be the best approach for studying neutrino oscillations. Ideally, the evaluation metric and the network loss function should be the sensitivity of the analysis to the oscillation parameters. However, it is not a simple problem to define a loss function that incorporates this into an event-by-event basis. Therefore, the sensitivity given by the $\Delta\chi^2$ between two oscillation hypotheses has to be computed when a training is done. The result is a $\Delta\chi^2$ value for each set of hyperparameters, and the set of hyperparameters that gives the lowest $\Delta\chi^2$ is the one that is selected.

Once the selection of the network hyperparameters is done, a full fit of the systematics for the oscillation analysis has to be done. This will be the final step to validate the energy estimate given by the network. This is done by applying the training model on the MC event sample containing neutrinos and atmospheric muons.

2. Methodology

2.1 Building the network

To perform the regression problem for energy estimation, a neural network using Keras with a TensorFlow backend is built [2]. The network consists of an input layer, followed by several dense hidden layers with an activation function, and a single output layer.

Track-like	**Shower-like**	**Trigger information**	**PID features**
Energy	Energy	Triggered hits	Track score
Fit likelihood	Fit likelihood	Triggered DOMs	Background score
3d event direction	3d event direction	Triggered DUs	
3d event position	3d event position		
Track length			

Table 1: Training features from the topology reconstructions, information on number of triggered hits and PID classification scores.

The inputs of the network are stated in Table 1, these include the standard energy estimates for the track hypothesis, the shower hypothesis, and the track length as energy proxy, information about the number of triggered hits, DOMs, and DUs, and scores from the particle identification (PID) tasks. The values of the energy estimates have a range from 1 GeV to 1 TeV, which is a very wide range of values for the network to learn from. This may cause difficulties to the network when reconstructing true energies around the energy range of interest for oscillations (5 - 40 GeV). The reason for this is that the network will focus more on the higher energies, as the loss function will be dominated by the higher energies. To avoid this, the energy estimates were input in logarithmic scale and the maximum energy for the training sample is set to be 100 GeV, this allows the network to learn from a wider range of values and to have a better performance for the energies in the region of interest. We simulate Charged Current (CC) and Neutral Current (NC) interacting events. The event types used for training are ν_μ CC, $\bar{\nu}_\mu$ CC, ν_e CC, $\bar{\nu}_e$ CC, ν_τ CC, $\bar{\nu}_\tau$ CC, ν NC, and $\bar{\nu}$ NC events. Additionally, at each layer, a batch normalization layer is applied to the input data. This is to normalize the input data to have a mean of zero and a standard deviation of one.

2.2 Network architecture

As a starting point, the number of nodes per layer was set to 32 and the number of hidden layers to 12. Without much tuning, the network was able to learn the energy distribution of the events. However, the network did not show any improvement over the standard methods when computing the sensitivity to the oscillation parameters. This was expected since the network was not trained to learn the oscillation effects, but rather to learn the energy distribution of the events. Therefore, the

events with the highest sensitivity to oscillations were not given more importance than the others and could eventually be regressed poorly by the network.

A skip connection architecture was implemented. This refers to an architecture breaking the sequential models by allowing layer outputs to skip connections and serve as input at a different layer on a later stage. The motivation behind this is to allow the network to learn the residual between the input and the output of the network, instead of learning the whole function. In our case, the input and output of the network are both energy estimates, and the residual between them is the energy resolution. Thus, we want the network to learn the energy resolution instead of the energy itself. This is done by concatenating the input energy estimates to the output of the network, and then train the network to learn the residual between them. With this method, the information about the energy estimates will not be washed out by mixing it with the other information in the network, and the network will be able to learn the energy resolution. As the energy estimate tends to perform differently depending on the type of event evaluated, it is a natural choice to include in the residuals the features related to the class selection given by the PID.

2.3 Weighting the events

In order to introduce some oscillation awareness during training, a novel method to set up the weights for training events was implemented. The method consists in giving more importance to events sensitive to oscillation effects. The usual weight of an event is given by $w = w(\Delta m^2_{31}, \theta_{23})$, where Δm^2_{31} and θ_{23} are the oscillation parameters we want to be sensitive to. One could compute the weights for events having a different set of oscillation parameters $w(\Delta m^2_{31}{}', \theta'_{23})$. The difference $\Delta w = |w(\Delta m^2_{31}, \theta_{23}) - w(\Delta m^2_{31}{}', \theta'_{23})|$ corresponds to the difference in oscillation effects for each event. For neutral current events the value of Δw will be zero, since they are unaffected by oscillations. For charged current events, Δw will be non-zero and will have a strong dependence on the direction and energy of the event.

During training, each event is given the following weight:

$$w_{osc} = K\Delta w + w. \tag{1}$$

Where K is a hyperparameter which sets the importance to the oscillation weights during the training. If K is large, the network will give more importance to events with oscillation sensitivity. If K is small, the most common events will be prioritized independent of their sensitivity oscillations.

2.4 Hyperparameter optimization

To further improve the performance of our neural network, the procedure of hyperparameter optimization to search for the optimal values of the hyperparameters was implemented. The choice for this purpose was the Optuna package in Python [3], which implements a Bayesian optimization algorithm (TPE) to efficiently search the hyperparameter space.

The selection of the hyperparameters to optimize are the following:

- Number of hidden layers: In the range of 8 to 64 with steps of 4.
- Number of neurons per hidden layer: In the range of 16 to 128, with steps of 16.
- Batch size: In the range of 32 to 254 with steps of 32.

- Learning rate: In the range of 10^{-7} to 10^{-5}, using a log-uniform distribution.
- Activation function for each hidden layer: The options to select the optimal activation function were PReLU, ReLU, LeakyReLU and ELU.
- The options for selecting the optimal loss function were mean squared error, mean absolute error and log cosh.
- Training features were divided into groups and the one performing the better was selected, groups of features are shown in Table 2.

	G1	G2	G3	G4	G5	G6	G7
Track-like energy	✓	✓	✓	✓	✓	✓	✓
Track-like likelihood	✓	✓	✓	✓	✓	✓	✓
Track-like track length	✓	✓	✓	✓	✓	✓	✓
Track-like x,y,z positions		✓		✓			✓
Track-like x,y,z directions			✓		✓	✓	✓
Shower-like energy	✓	✓	✓	✓	✓	✓	✓
Shower-like likelihood	✓	✓	✓	✓	✓	✓	✓
Shower-like x,y,z positions		✓		✓			✓
Shower-like x,y,z directions			✓		✓	✓	✓
Triggered hits	✓	✓	✓	✓	✓	✓	✓
Triggered DOMs				✓	✓	✓	✓
Triggered DUs				✓	✓	✓	✓
Track score						✓	✓
Background score						✓	✓

Table 2: Group of features tested for the hyperparameter optimization procedure.

The hyperparameters were optimized using the MSE as a metric. The optimization was done using the training sample containing 1.48M neutrino CC and NC events, and the performance of the network was evaluated using the validation sample of 396k neutrino CC and NC events.

Hyperparameter	**Value**
Activation function	ELU
Osci. w normalization K	103188.39
Learning rate	8.009e-06
Batch size	64
Number of nodes per layer	128
Number of hidden layers	20
Loss function	Mean Squared Error
Feature group	G6

Table 3: Table of Hyperparameters of the models trained and selected with the highest $\Delta\chi^2$ value.

It is difficult to assess if a reconstruction is good for computing sensitivities to oscillation parameters. The standard way to compare energy reconstructions is to look at the distribution of reconstructed energy versus true energy i.e. the energy response function. However, this is not

enough to tell whether the reconstruction is good or not, since the distribution could be centered around the diagonal but with a large spread. As the response function is not a single number, it cannot be used to define a metric for our purposes. In particular, we care about having a correct energy reconstruction for oscillating events, since they are the ones used to compute the sensitivity to oscillation parameters. The best energy estimate may depend on the specific task one might want to accomplish. Therefore, we choose the sensitivity to oscillation as our ultimate metric of performance for this work. This is done computing the sensitivity to oscillation parameters using the energy estimate given by the DNN, and comparing it with the sensitivity using the standard energy estimates.

The standard way to do this is by computing the $\Delta\chi^2$ between two sets of oscillation parameters using our internal oscillation analysis framework [4]. The direct use of this framework during the training as part of a loss function is not possible. Also loading the data into the framework after each training epoch is not feasible, since it would be too slow. For this reason, we use a custom approximate implementation of the sensitivity calculation which can compute $\Delta\chi^2$ values directly from the obtained reconstructed energies at the end of each training. This allows to compare different models, and select the one with the best performance. The $\Delta\chi^2$ sensitivity is computed for different topology classes of events (High Purity Tracks, Low Purity Tracks and Showers) [5]. The model selected is the one with the best performance for the sum of the $\Delta\chi^2$ of the three classes.

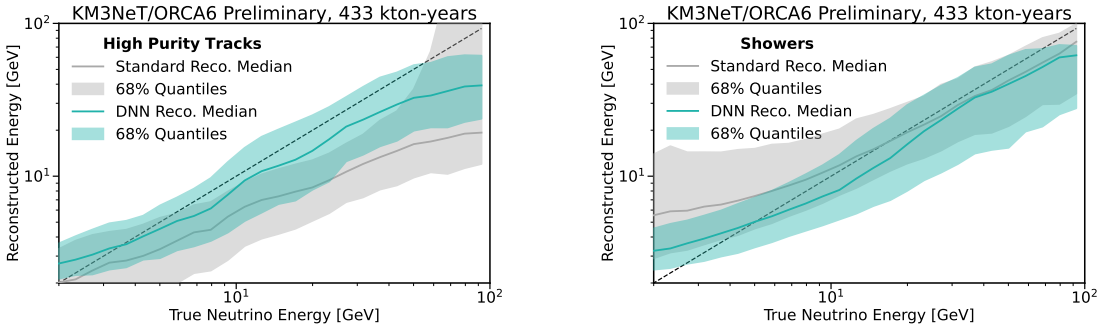

(a) High Purity Tracks class

(b) Showers class

Figure 1: Energy response functions for different classes of neutrino events. Events are reconstructed using the standard method and the DNN to compare.

3. Results and discussion

After training the neural network and selecting the optimal hyperparameters, the performance of the network is evaluated.

3.1 Energy response function

The energy response function of the neural network is compared with the standard reconstruction method in Figure 1, where we show the energy resolution for the different classes of events.

The energy estimate given by the DNN shows a distribution with less bias than the standard reconstruction method. Additionally, the energy for the track events saturates eventually at a given energy for both energy estimates. This is a consequence of the finite size of the detector which may not contain the full energy deposition of the events. The muon produced in the interaction will leave the detector without fully depositing all its energy. For the case of the DNN, we see this saturation to occur at a higher reconstructed energy, possibly meaning the DNN is able to get information from the hadronic shower given by the triggered hits to correctly reconstruct the energy of the event. This effect is particularly useful to prevent the presence of events with high true energy from polluting the sample of reconstructed energies around the oscillation regime.

3.2 Sensitivity to oscillation parameters

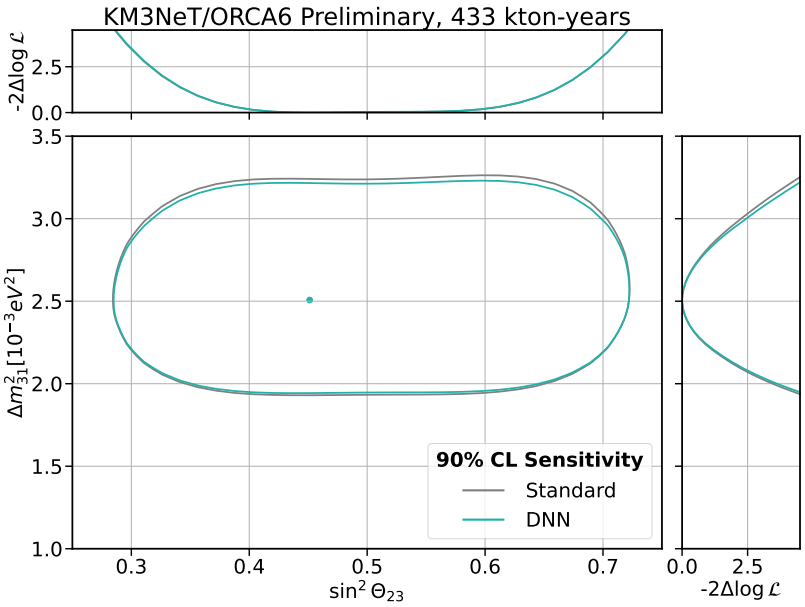

Figure 2: Contour at 90% CL of ORCA6 sensitivity to oscillation parameters θ_{23} and Δm^2_{32} using the DNN reconstructed energy compared with the standard energy estimates.

The performance of the network is evaluated by computing the sensitivity to oscillation parameters as a $\Delta\chi^2$ using the reconstructed energy and by comparing with the standard energy estimates. Results are shown in Figure 2. At every point in the contour the log-likelihood is minimized relative to all nuisance parameters defined for the main oscillation analysis of the experiment [5]. The figure shows that the network leads to a better performance in constraining the value of Δm^2_{32}. For the case of θ_{23}, the gain is negligible.

In order to assess the gain of using the DNN for the analyses, we compute the exposure needed to attain the same values of the errors on the oscillation parameters. Results are shown in Figure 3. The figure shows that the better precision of the DNN for the Δm^2_{32} parameter is equivalent to having 12% more exposure, while for the $\sin^2(\theta_{23})$ parameter it is equivalent to having 2% more exposure.

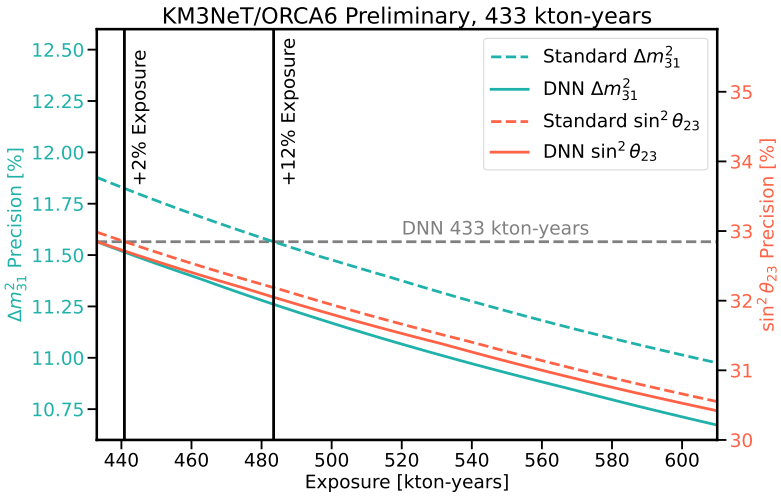

Figure 3: Precision to oscillation parameters $\sin^2\theta_{23}$ and Δm^2_{32} as a function of exposure in kton-years for the DNN and the standard energy estimates.

3.3 Summary

Using a Deep Neural Network combining the energy estimates from three standard reconstruction methods plus additional topological information of the events allows to improve the performance of the energy reconstruction of an event. This improvement is translated into a better sensitivity to oscillation parameters, and a gain in precision for the same exposure. Additionally, the reconstructed energy has less bias than the standard reconstruction methods. This method highlights the importance of having a reconstruction that considers the different topologies of a neutrino interaction. This tool will continue to be improved and tested on the different physics analyses, including BSM scenarios within the collaboration. Future work will test different sample selections and a wider scan of training features to look for improvements on the sensitivity to oscillations.

References

[1] S. Adrian-Martinez, M. Ageron, F. Aharonian, S. Aiello, A. Albert, F. Ameli, E. Anassontzis, M. Andre, G. Androulakis, M. Anghinolfi, *et al.*, "Letter of intent for KM3NeT 2.0," *Journal of Physics G: Nuclear and Particle Physics*, vol. 43, no. 8, p. 084001, 2016.

[2] F. Chollet *et al.*, "Keras." https://keras.io, 2015.

[3] T. Akiba, S. Sano, T. Yanase, T. Ohta, and M. Koyama, "Optuna: A Next-generation Hyperparameter Optimization Framework," in *Proceedings of the 25th ACM SIGKDD International Conference on Knowledge Discovery and Data Mining*, 2019.

[4] S. Bourret, *Neutrino oscillations and earth tomography with KM3NeT-ORCA*. PhD thesis, Université Sorbonne Paris Cité, 2018.

[5] V. Carretero. PoS(ICRC2023)996, 2023.

Full Authors List: The KM3NeT Collaboration

S. Aiello[a], A. Albert[b,bd], S. Alves Garre[c], Z. Aly[d], A. Ambrosone[f,e], F. Ameli[g], M. Andre[h], E. Androutsou[i], M. Anguita[j], L. Aphecetche[k], M. Ardid[l], S. Ardid[l], H. Atmani[m], J. Aublin[n], L. Bailly-Salins[o], Z. Bardačová[q,p], B. Baret[n], A. Bariego-Quintana[c], S. Basegmez du Pree[r], Y. Becherini[n], M. Bendahman[m,n], F. Benfenati[t,s], M. Benhassi[u,e], D. M. Benoit[v], E. Berbee[r], V. Bertin[d], S. Biagi[w], M. Boettcher[x], D. Bonanno[w], J. Boumaaza[m], M. Bouta[y], M. Bouwhuis[r], C. Bozza[z,e], R. M. Bozza[f,e], H.Brânzaş[aa], F. Bretaudeau[k], R. Bruijn[ab,r], J. Brunner[d], R. Bruno[a], E. Buis[ac,r], R. Buompane[u,e], J. Busto[d], B. Caiffi[ad], D. Calvo[c], S. Campion[g,ae], A. Capone[g,ae], F. Carenini[t,s], V. Carretero[c], T. Cartraud[n], P. Castaldi[af,s], V. Cecchini[c], S. Celli[g,ae], L. Cerisy[d], M. Chabab[ag], M. Chadolias[ah], A. Chen[ai], S. Cherubini[aj,w], T. Chiarusi[s], M. Circella[ak], R. Cocimano[w], J. A. B. Coelho[n], A. Coleiro[n], R. Coniglione[w] P. Coyle[d], A. Creusot[n], A. Cruz[al], G. Cuttone[w], R. Dallier[k], Y. Darras[ah], A. De Benedittis[e], B. De Martino[d], V. Decoene[k], R. Del Burgo[e], U. M. Di Cerbo[e], L. S. Di Mauro[w], I. Di Palma[g,ae], A. F. Díaz[j], C. Diaz[j], D. Diego-Tortosa[w], C. Distefano[w], A. Domi[ah], C. Donzaud[n], D. Dornic[d], M. Dörr[am], E. Drakopoulou[i], D. Drouhin[b,bd], R. Dvornický[q], T. Eberl[ah], E. Eckerová[q,p], A. Eddymaoui[m], T. van Eeden[r], M. Eff[n], D. van Eijk[r], I. El Bojaddaini[y], S. El Hedri[n], A. Enzenhöfer[d], G. Ferrara[w], M. D. Filipović[an], F. Filippini[t,s], D. Franciotti[w], L. A. Fusco[z,e], J. Gabriel[ao], S. Gagliardini[g], T. Gal[ah], J. García Méndez[l], A. Garcia Soto[c], C. Gatius Oliver[r], N. Geißelbrecht[ah], H. Ghaddari[y], L. Gialanella[e,u], B. K. Gibson[v], E. Giorgio[w], I. Goos[n], D. Goupilliere[o], S. R. Gozzini[c], R. Gracia[ah], K. Graf[ah], C. Guidi[ap,ad], B. Guillon[o], M. Gutiérrez[aq], H. van Haren[ar], A. Heijboer[r], A. Hekalo[am], L. Hennig[ah], J. J. Hernández-Rey[c], F. Huang[d], W. Idrissi Ibnsalih[e], G. Illuminati[s], C. W. James[al], M. de Jong[as,r], P. de Jong[ab,r], B. J. Jung[r], P. Kalaczyński[at,be], O. Kalekin[ah], U. F. Katz[ah], N. R. Khan Chowdhury[c], A. Khatun[q], G. Kistauri[av,au], C. Kopper[ah], A. Kouchner[aw,n], V. Kulikovskiy[ad], R. Kvatadze[av], M. Labalme[o], R. Lahmann[ah], G. Larosa[w], C. Lastoria[d], A. Lazo[c], S. Le Stum[d], G. Lehaut[o], E. Leonora[a], N. Lessing[c], G. Levi[t,s], M. Lindsey Clark[n], F. Longhitano[a], J. Majumdar[r], L. Malerba[ad], F. Mamedov[p], J. Mańczak[c], A. Manfreda[e], M. Marconi[ap,ad], A. Margiotta[t,s], A. Marinelli[e,f], C. Markou[i], L. Martin[k], J. A. Martínez-Mora[l], F. Marzaioli[u,e], M. Mastrodicasa[ae,g], S. Mastroianni[e], S. Miccichè[w], G. Miele[f,e], P. Migliozzi[e], E. Migneco[w], M. L. Mitsou[e], C. M. Mollo[e], L. Morales-Gallegos[u,e], C. Morley-Wong[al], A. Moussa[y], I. Mozun Mateo[ay,ax], R. Muller[r], M. R. Musone[e,u], M. Musumeci[w], L. Nauta[r], S. Navas[aq], A. Nayerhoda[ak], C. A. Nicolau[g], B. Nkosi[ai], B. Ó Fearraigh[ab,r], V. Oliviero[f,e], A. Orlando[w], E. Oukacha[n], D. Paesani[w], J. Palacios González[c], G. Papalashvili[au], V. Parisi[ap,ad], E.J. Pastor Gomez[c], A. M. Păun[aa], G. E. Păvălaş[aa], S. Peña Martínez[n], M. Perrin-Terrin[d], J. Perronnel[o], V. Pestel[ay], R. Pestes[n], P. Piattelli[w], C. Poirè[z,e], V. Popa[aa], T. Pradier[b], S. Pulvirenti[w], G. Quéméner[o], C. Quiroz[l], U. Rahaman[c], N. Randazzo[a], R. Randriatoamanana[k], S. Razzaque[az], I. C. Rea[e], D. Real[c], S. Reck[ah], G. Riccobene[w], J. Robinson[x], A. Romanov[ap,ad], A. Šaina[c], F. Salesa Greus[c], D. F. E. Samtleben[as,r], A. Sánchez Losa[c,ak], S. Sanfilippo[w], M. Sanguineti[ap,ad], C. Santonastaso[ba,e], D. Santonocito[w], P. Sapienza[w], J. Schnabel[ah], J. Schumann[ah], H. M. Schutte[x], J. Seneca[r], N. Sennan[y], B. Setter[ah], I. Sgura[ak], R. Shanidze[au], Y. Shitov[p], F. Šimkovic[q], A. Simonelli[e], A. Sinopoulou[a], M.V. Smirnov[ah], B. Spisso[e], M. Spurio[t,s], D. Stavropoulos[i], I. Štekl[p], M. Taiuti[ap,ad], Y. Tayalati[m], H. Tedjditi[ad], H. Thiersen[x], I. Tosta e Melo[a,aj], B. Trocmé[n], V. Tsourapis[i], E. Tzamariudaki[i], A. Vacheret[o], V. Valsecchi[w], V. Van Elewyck[aw,n], G. Vannoye[d], G. Vasileiadis[bb], F. Vazquez de Sola[r], C. Verilhac[n], A. Veutro[g,ae], S. Viola[w], D. Vivolo[u,e], J. Wilms[bc], E. de Wolf[ab,r], H. Yepes-Ramirez[l], G. Zarpapis[i], S. Zavatarelli[ad], A. Zegarelli[g,ae], D. Zito[w], J. D. Zornoza[c], J. Zúñiga[c], and N. Zywucka[x].

[a] INFN, Sezione di Catania, Via Santa Sofia 64, Catania, 95123 Italy
[b] Université de Strasbourg, CNRS, IPHC UMR 7178, F-67000 Strasbourg, France
[c] IFIC - Instituto de Física Corpuscular (CSIC - Universitat de València), c/Catedrático José Beltrán, 2, 46980 Paterna, Valencia, Spain
[d] Aix Marseille Univ, CNRS/IN2P3, CPPM, Marseille, France
[e] INFN, Sezione di Napoli, Complesso Universitario di Monte S. Angelo, Via Cintia ed. G, Napoli, 80126 Italy
[f] Università di Napoli "Federico II", Dip. Scienze Fisiche "E. Pancini", Complesso Universitario di Monte S. Angelo, Via Cintia ed. G, Napoli, 80126 Italy
[g] INFN, Sezione di Roma, Piazzale Aldo Moro 2, Roma, 00185 Italy
[h] Universitat Politècnica de Catalunya, Laboratori d'Aplicacions Bioacústiques, Centre Tecnològic de Vilanova i la Geltrú, Avda. Rambla Exposició, s/n, Vilanova i la Geltrú, 08800 Spain
[i] NCSR Demokritos, Institute of Nuclear and Particle Physics, Ag. Paraskevi Attikis, Athens, 15310 Greece
[j] University of Granada, Dept. of Computer Architecture and Technology/CITIC, 18071 Granada, Spain
[k] Subatech, IMT Atlantique, IN2P3-CNRS, Université de Nantes, 4 rue Alfred Kastler - La Chantrerie, Nantes, BP 20722 44307 France
[l] Universitat Politècnica de València, Instituto de Investigación para la Gestión Integrada de las Zonas Costeras, C/ Paranimf, 1, Gandia, 46730 Spain
[m] University Mohammed V in Rabat, Faculty of Sciences, 4 av. Ibn Battouta, B.P. 1014, R.P. 10000 Rabat, Morocco
[n] Université Paris Cité, CNRS, Astroparticule et Cosmologie, F-75013 Paris, France
[o] LPC CAEN, Normandie Univ, ENSICAEN, UNICAEN, CNRS/IN2P3, 6 boulevard Maréchal Juin, Caen, 14050 France
[p] Czech Technical University in Prague, Institute of Experimental and Applied Physics, Husova 240/5, Prague, 110 00 Czech Republic
[q] Comenius University in Bratislava, Department of Nuclear Physics and Biophysics, Mlynska dolina F1, Bratislava, 842 48 Slovak Republic
[r] Nikhef, National Institute for Subatomic Physics, PO Box 41882, Amsterdam, 1009 DB Netherlands
[s] INFN, Sezione di Bologna, v.le C. Berti-Pichat, 6/2, Bologna, 40127 Italy
[t] Università di Bologna, Dipartimento di Fisica e Astronomia, v.le C. Berti-Pichat, 6/2, Bologna, 40127 Italy
[u] Università degli Studi della Campania "Luigi Vanvitelli", Dipartimento di Matematica e Fisica, viale Lincoln 5, Caserta, 81100 Italy
[v] E. A. Milne Centre for Astrophysics, University of Hull, Hull, HU6 7RX, United Kingdom

[w] INFN, Laboratori Nazionali del Sud, Via S. Sofia 62, Catania, 95123 Italy
[x] North-West University, Centre for Space Research, Private Bag X6001, Potchefstroom, 2520 South Africa
[y] University Mohammed I, Faculty of Sciences, BV Mohammed VI, B.P. 717, R.P. 60000 Oujda, Morocco
[z] Università di Salerno e INFN Gruppo Collegato di Salerno, Dipartimento di Fisica, Via Giovanni Paolo II 132, Fisciano, 84084 Italy
[aa] ISS, Atomistilor 409, Măgurele, RO-077125 Romania
[ab] University of Amsterdam, Institute of Physics/IHEF, PO Box 94216, Amsterdam, 1090 GE Netherlands
[ac] TNO, Technical Sciences, PO Box 155, Delft, 2600 AD Netherlands
[ad] INFN, Sezione di Genova, Via Dodecaneso 33, Genova, 16146 Italy
[ae] Università La Sapienza, Dipartimento di Fisica, Piazzale Aldo Moro 2, Roma, 00185 Italy
[af] Università di Bologna, Dipartimento di Ingegneria dell'Energia Elettrica e dell'Informazione "Guglielmo Marconi", Via dell'Università 50, Cesena, 47521 Italia
[ag] Cadi Ayyad University, Physics Department, Faculty of Science Semlalia, Av. My Abdellah, P.O.B. 2390, Marrakech, 40000 Morocco
[ah] Friedrich-Alexander-Universität Erlangen-Nürnberg (FAU), Erlangen Centre for Astroparticle Physics, Nikolaus-Fiebiger-Straße 2, 91058 Erlangen, Germany
[ai] University of the Witwatersrand, School of Physics, Private Bag 3, Johannesburg, Wits 2050 South Africa
[aj] Università di Catania, Dipartimento di Fisica e Astronomia "Ettore Majorana", Via Santa Sofia 64, Catania, 95123 Italy
[ak] INFN, Sezione di Bari, via Orabona, 4, Bari, 70125 Italy
[al] International Centre for Radio Astronomy Research, Curtin University, Bentley, WA 6102, Australia
[am] University Würzburg, Emil-Fischer-Straße 31, Würzburg, 97074 Germany
[an] Western Sydney University, School of Computing, Engineering and Mathematics, Locked Bag 1797, Penrith, NSW 2751 Australia
[ao] IN2P3, LPC, Campus des Cézeaux 24, avenue des Landais BP 80026, Aubière Cedex, 63171 France
[ap] Università di Genova, Via Dodecaneso 33, Genova, 16146 Italy
[aq] University of Granada, Dpto. de Física Teórica y del Cosmos & C.A.F.P.E., 18071 Granada, Spain
[ar] NIOZ (Royal Netherlands Institute for Sea Research), PO Box 59, Den Burg, Texel, 1790 AB, the Netherlands
[as] Leiden University, Leiden Institute of Physics, PO Box 9504, Leiden, 2300 RA Netherlands
[at] National Centre for Nuclear Research, 02-093 Warsaw, Poland
[au] Tbilisi State University, Department of Physics, 3, Chavchavadze Ave., Tbilisi, 0179 Georgia
[av] The University of Georgia, Institute of Physics, Kostava str. 77, Tbilisi, 0171 Georgia
[aw] Institut Universitaire de France, 1 rue Descartes, Paris, 75005 France
[ax] IN2P3, 3, Rue Michel-Ange, Paris 16, 75794 France
[ay] LPC, Campus des Cézeaux 24, avenue des Landais BP 80026, Aubière Cedex, 63171 France
[az] University of Johannesburg, Department Physics, PO Box 524, Auckland Park, 2006 South Africa
[ba] Università degli Studi della Campania "Luigi Vanvitelli", CAPACITY, Laboratorio CIRCE - Dip. Di Matematica e Fisica - Viale Carlo III di Borbone 153, San Nicola La Strada, 81020 Italy
[bb] Laboratoire Univers et Particules de Montpellier, Place Eugène Bataillon - CC 72, Montpellier Cédex 05, 34095 France
[bc] Friedrich-Alexander-Universität Erlangen-Nürnberg (FAU), Remeis Sternwarte, Sternwartstraße 7, 96049 Bamberg, Germany
[bd] Université de Haute Alsace, rue des Frères Lumière, 68093 Mulhouse Cedex, France
[be] AstroCeNT, Nicolaus Copernicus Astronomical Center, Polish Academy of Sciences, Rektorska 4, Warsaw, 00-614 Poland

Acknowledgements

The authors acknowledge the financial support of the funding agencies: Agence Nationale de la Recherche (contract ANR-15-CE31-0020), Centre National de la Recherche Scientifique (CNRS), Commission Européenne (FEDER fund and Marie Curie Program), LabEx UnivEarthS (ANR-10-LABX-0023 and ANR-18-IDEX-0001), Paris Île-de-France Region, France; Shota Rustaveli National Science Foundation of Georgia (SRNSFG, FR-22-13708), Georgia; The General Secretariat of Research and Innovation (GSRI), Greece Istituto Nazionale di Fisica Nucleare (INFN), Ministero dell'Università e della Ricerca (MIUR), PRIN 2017 program (Grant NAT-NET 2017W4HA7S) Italy; Ministry of Higher Education, Scientific Research and Innovation, Morocco, and the Arab Fund for Economic and Social Development, Kuwait; Nederlandse organisatie voor Wetenschappelijk Onderzoek (NWO), the Netherlands; The National Science Centre, Poland (2021/41/N/ST2/01177); The grant "AstroCeNT: Particle Astrophysics Science and Technology Centre", carried out within the International Research Agendas programme of the Foundation for Polish Science financed by the European Union under the European Regional Development Fund; National Authority for Scientific Research (ANCS), Romania; Grants PID2021-124591NB-C41, -C42, -C43 funded by MCIN/AEI/ 10.13039/501100011033 and, as appropriate, by "ERDF A way of making Europe", by the "European Union" or by the "European Union NextGenerationEU/PRTR", Programa de Planes Complementarios I+D+I (refs. ASFAE/2022/023, ASFAE/2022/014), Programa Prometeo (PROMETEO/2020/019) and GenT (refs. CIDEGENT/2018/034, /2019/043, /2020/049. /2021/23) of the Generalitat Valenciana, Junta de Andalucía (ref. SOMM17/6104/UGR, P18-FR-5057), EU: MSC program (ref. 101025085), Programa María Zambrano (Spanish Ministry of Universities, funded by the European Union, NextGenerationEU), Spain; The European Union's Horizon 2020 Research and Innovation Programme (ChETEC-INFRA - Project no. 101008324).